DALTON
FULL PAPER

Structure and bonding of bisaquamercury(II) and trisaquathallium(III) trifluoromethanesulfonate †

Alireza Molla-Abbassi,[a] Lars Eriksson,[a] János Mink,[b,c] Ingmar Persson,[d] Magnus Sandström,*[a] Mikhail Skripkin,[e] Ann-Sofi Ullström[d] and Patric Lindqvist-Reis[f]

[a] *Structural Chemistry, Stockholm University, SE-106 91 Stockholm, Sweden*
[b] *Institute of Isotopes and Surface Chemistry, Chemical Research Center of the Hungarian Academy of Sciences, P.O. Box 77, H-1525, Budapest, Hungary*
[c] *Analytical Chemistry Department, University of Veszprém, P.O. Box 158, H-8201, Veszprém, Hungary*
[d] *Department of Chemistry, Swedish University of Agricultural Sciences, P.O. Box 7015, SE-750 07 Uppsala, Sweden*
[e] *St. Petersburg State University, Department of Chemistry, Universitetskii pr. 2, SU-198904, St. Petersburg, Russia*
[f] *Institut für Nukleare Entsorgung, Forschungszentrum Karlsruhe, P.O. Box 3640, D-76021, Karlsruhe, Germany*

Received 21st June 2002, Accepted 20th September 2002
First published as an Advance Article on the web 29th October 2002

The structure and bonding in bisaquamercury(II) trifluoromethanesulfonate, $[Hg(OH_2)_2(CF_3SO_3)_2]_\infty$, and trisaquathallium(III) trifluoromethanesulfonate, $[Tl(OH_2)_3(CF_3SO_3)_3]$, have been studied by means of single-crystal X-ray diffraction, EXAFS and vibrational spectroscopy. The crystal structure of bisaquamercury(II) trifluoromethanesulfonate shows an unusual connectivity pattern. The mercury(II) ion strongly binds two water molecules axially with the Hg–O bond distance 2.11 Å, and four oxygen atoms from four trifluoromethanesulfonate ions complete a tetragonally compressed octahedral coordination geometry, at the mean Hg–O distance 2.53 Å. Two trifluoromethanesulfonate ions form double bridges between the bisaquamercury(II) entities giving rise to infinite $>Hg(OH_2)_2<(CF_3SO_3)_2>Hg(OH_2)_2<$ chains. The parallel chains are held together in layers by relatively strong hydrogen bonds with O(–H) ··· O distances in the range 2.688(9)–2.735(9) Å. The O–D stretching vibrational frequencies of the hydrogen bonds in the partly deuterated compound occur in a broad band at about 2400 cm^{-1}, bandwidth *ca.* 170 cm^{-1}. The layers are connected only *via* van der Waals interactions between the protruding CF_3 groups, consistent with the fragile sheet-like structure of the crystalline compound. Trisaquathallium(III) trifluoromethanesulfonate crystallises as molecular complexes where each thallium(III) ion binds three water molecules and three oxygen atoms from trifluoromethanesulfonate ions, with Tl–O bond distances in the range 2.18–2.24 Å. A hydrogen bond network between the water molecules and trifluoromethanesulfonate ions with O(–H) ··· O distances in the range 2.65(1)–2.80(1) Å holds the structure together. Raman and infrared spectra have been recorded and analysed. The changes in force constants and vibrational frequencies have been correlated with bond lengths for the S–O bond in the coordinated trifluoromethanesulfonate ion and for the Hg–O and Tl–O bonds, also including the hexaaquaions in the comparisons.

Introduction

The mercury(II) ion is six-coordinated in the solid solvates of water, dimethylsulfoxide, pyridine-1-oxide and pyridine,[1–6] as well as in aqueous and dimethylsulfoxide solution.[6,7] The solid solvates $[Hg(OH_2)_6](ClO_4)_2$, $[Hg(OS(CH_3)_2)_6](CF_3SO_3)_2$ and $[Hg(ONC_5H_5)_6](ClO_4)_2$, crystallize in high symmetry space groups,[1,3,4] in which the solvated mercury(II) ions appear as near-regular octahedral complexes with equidistant Hg–O bonds. However, EXAFS studies show the distribution of the Hg–O bond distances to be much wider, both in the solid state and in solution, than usual for a divalent metal ion.[6] The crystal structures of the $[Hg(OS(CH_3)_2)_6](ClO_4)_2$ and $[Hg(NC_5H_5)_6](CF_3SO_3)_2$ compounds display centrosymmetric complexes with the four equatorial Hg–O/N bonds significantly shorter, *ca.* 0.05 Å, than the axial ones,[2,5] probably due to a pseudo (or second order) Jahn-Teller (SOJT) effect.[8] Thus, it seems that mercury(II) in all octahedral complexes studied so far is affected by a SOJT effect, leading to distortions in the coordination. In very soft solvents (with values of the softness parameter $D_S >\sim 50$),[9] the SOJT destabilization of the octahedral coordination geometry, *i.e.* by vibronic coupling of near-degenerate electronic states,[8] seems to be the main reason why the solvated mercury(II) ion changes to tetrahedral four-coordination as found for *N,N*-dimethylthioformamide ($D_S = 56$)[10] and liquid ammonia ($D_S = 69$).[11]

Hydrated and dimethylsulfoxide solvated thallium(III) ions are reported with regular octahedral coordination in the solid state and in solution,[12–15] and the six equidistant Tl–O bonds do not display any sign of SOJT effects in the solid compounds. However, some hexabromothallate(III) complexes show distinct tetragonal elongation or compression of the octahedral structure in the solid state.[16] Thus, for thallium(III) complexes it seems that typically soft ligands are required to create conditions that allow vibronic mixing of molecular orbitals strong

† Electronic supplementary information (ESI) available: symmetry coordinates for **1** and **2**; observed and calculated frequencies and potential energy distribution for $CF_3SO_3^-$, **1** and **2**; X-ray absorption edge structure for **1**, $[Hg(OH_2)_6](ClO_4)_2$, $[Hg(NH_3)_4](ClO_4)_2$, **2** and $[Tl(OH_2)_6]^{3+}$. See http://www.rsc.org/suppdata/dt/b2/b206021n/

DOI: 10.1039/b206021n

enough to distort the octahedral ligand configuration, while for the isoelectronic mercury(II) ion oxygen donor ligands are sufficient. The thallium(III) ion is spontaneously reduced to thallium(I) in the sulfur donor solvent *N,N*-dimethylthioformamide,[17] while preliminary results indicate that the thallium(III) ion is tetrahedrally four-coordinated in liquid ammonia.[11]

To further evaluate the difference in SOJT effects for the d^{10} ions mercury(II) and thallium(III) with fairly hard oxygen donor ligands, trifluoromethanesulfonate hydrates were crystallised and characterised by crystallography and vibrational spectroscopy in the present work. With the intention to facilitate the evaluation of these rather subtle effects on the metal ion coordination, trifluoromethanesulfonate was chosen as counter ion because its elongated shape less often causes crystallographic disorder, or a space group with apparently too high symmetry, than perchlorate.[6] Trifluoromethanesulfonate salts of many metal ions are used as catalysts for a number of useful reactions in organic synthesis, both in organic and also mixed aqueous media, and are often recommended for preparation of solutions of metal ions in organic solvents, because of the risk of explosions with perchlorate. Even though these two anions often are assumed to have similar non-coordinating properties in solution, it soon became clear in the current study that in the solid state their different properties can cause substantial differences in the coordination chemistry of the metal ions.

Table 1 Crystallographic data for **1** and **2**

	1	**2**
Formula	$C_2H_4F_6O_8S_2Hg$	$C_3H_6F_9O_{12}S_3Tl$
M	534.76	705.63
Crystal system	Triclinic	Monoclinic
Space group	$P\bar{1}$ (No.2)	$C\,2/c$ (No.15)
a/Å	7.878(3)	26.990(9)
b/Å	7.977(3)	13.376(4)
c/Å	9.831(4)	19.133(6)
α/°	98.339(7)	90
β/°	98.779(7)	149.737(18)
γ/°	96.104(7)	90
V/Å3	598.9(4)	3481(2)
T/K	295	293
Z	2	8
D_c/g cm^{-3}	2.966	2.693
μ(Mo–Kα)/mm^{-1}	13.31	9.79
Measured reflections	3726	7288
Unique reflections	2572 (R_{int} = 0.0916)	1822 (R_{int} = 0.0796)
Observed reflections	2373	1350
Final *R*1, w*R*2[$I > 2\sigma(I)$][a]	0.0442, 0.1278	0.0361, 0.0768
(all data)	0.0478, 0.1309	0.0540, 0.0795

[a] *R* values are defined as: $R_1 = \Sigma||F_o|-|F_c||/\Sigma|F_o|$ $wR_2 = [\Sigma[w(F_o^2 - F_c^2)^2] / \Sigma[w(F_o^2)^2]]^{1/2}$.

Experimental

Chemicals

Bisaquamercury(II) trifluoromethanesulfonate, $[Hg(OH_2)_2(O_3SCF_3)_2]_\infty$, **1**, was obtained by dissolving mercury(II) oxide in aqueous (20 volume%) trifluoromethanesulfonic acid (Riedel de-Haën). Slow evaporation yielded colourless fragile crystals in thin flakes. Trisaquathallium(III) trifluoromethanesulfonate, $[Tl(OH_2)_3(O_3SCF_3)_3]$, **2**, was prepared as described elsewhere.[17] Note that all mercury(II) and thallium(III) compounds are toxic and should be handled with care.

X-Ray crystallography

The data collections were made at ambient temperature. A STOE imaging-plate diffractometer[18a] was used for a small crystal of **2**, 0.12 × 0.10 × 0.03 mm, enclosed in a thin-walled glass capillary. The crystal to imaging plate distance was 100 mm, and ϕ-scan was used from 0 to 200 with 1.5 step. The transmission factors varied between 0.303 and 0.734.

A Bruker SMART platform equipped with a CCD area detector,[18b] was used for a flat crystal of **1**, 0.29 × 0.18 × 0.09 mm. A hemisphere of data (1295 frames) was collected using the omega scan method (0.3° frame width) and a crystal to detector distance of 50 mm. The first 50 frames were remeasured at the end of the data collection to monitor crystal and instrument stability, and showed the intensity variation to be negligible. However, the transmission factors showed large variations for the crystal, between 0.021 and 0.295. The absorption correction was performed with the program X-RED using numerical integration and calculation of transmission factors, and the shape of the crystal was verified with the program X-SHAPE.[19] Even when absorption effects heavily affect the reflection data there are usually no additional problems in solving the crystal structure. However, the derived quantities, *e.g.* the distances of the model may be severely influenced by the systematic errors, and reliable absorption corrections are highly desirable for precisely derived parameters. In the present case, the e.s.d.s became 50% smaller when using the absorption corrected data, and the shortest Hg–O distances changed by about 0.016 Å to the current values.

The structures were solved by utilising direct methods in the SHELXS-97 program package,[20] followed by full-matrix least squares refinements on F^2. Non-hydrogen atoms were treated anisotropically. The hydrogen atoms of the water molecules were located from the residual density map and refined with a tight restraint of the O–H bond length of 0.96(1) Å, i.e. the estimated standard deviation 0.01 Å, while keeping the H ··· H distance at a value corresponding to the H–O–H angle 104.5°. In addition, the hydrogen bond H ··· O distances to the acceptor oxygen atoms were restrained with much looser e.s.d. values, 0.05 Å. This way of modeling was chosen to allow reorientation of almost rigid water molecules in a robust way, as no riding atom model is available in SHELXL97 for water molecules, except the general fragment model.

General crystal and experimental data are summarised in Table 1, the metal ion–oxygen bond distances displayed in Figs. 1 and 6, and the hydrogen bond distances are collected in Table 2.

CCDC reference numbers 188198 and 188199.

See http://www.rsc.org/suppdata/dt/b2/b206021n/ for crystallographic data in CIF or other electronic format.

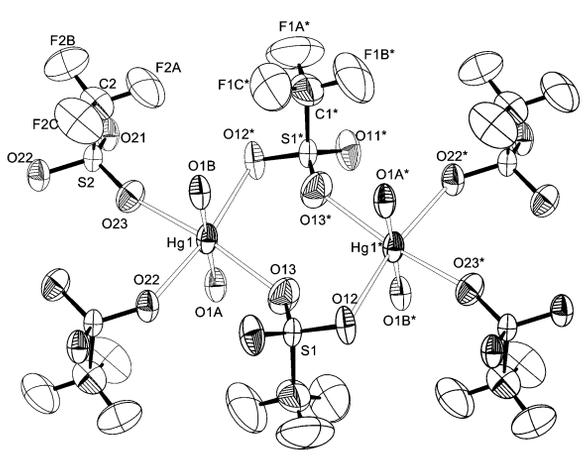

Fig. 1 The strongly bonded $Hg(OH_2)_2^{2+}$ entities (Hg–O1A 2.113(7) Å and Hg–O1B 2.114(7) Å) joined by double bridges (unfilled Hg–O bonds) of trifluoromethanesulfonate ions into $[Hg(OH_2)_2(O_3SCF_3)_2]_\infty$ chains: Hg–O12[(i)] 2.660(7), Hg–O13 2.523(9), Hg–O22 2.463(6) and Hg–O23[(ii)] 2.491(7) Å. Thermal ellipsoids at 50 % probability level. Symmetry codes: (i) $-x + 1, -y + 1, -z + 1$; (ii) $-x, -y, -z + 1$ and in figure (*) $-x, -y, -z$.

Table 2 Hydrogen bond data (distances in Å with e.s.d.s in parentheses, angles in degrees). for the mercury(II) hydrate (**1**) and the thallium(III) hydrate (**2**)

D	H	A	D–H[a]	H ··· A[a]	D ··· A	D–H ··· A	Symmetry operation for A
1							
O1A	H1AA	O21	0.96	1.80(1)	2.720(9)	158	$x + 1, y, z$
O1A	H1AB	O12	0.96	1.83(1)	2.708(9)	150	$x, y - 1, z$
O1B	H1BA	O21	0.96	1.78(1)	2.735(9)	166	$-x, -y + 1, -z + 1$
O1B	H1BB	O11	0.96	1.75(1)	2.688(9)	164	$-x, -y + 1, -z + 1$
2							
O1	H11	O22	0.96	1.70(1)	2.661(14)	174	$x + 1/2, -y + 1/2, z + 1/2$
O1	H12	O32	0.96	1.85(1)	2.803(12)	171	$-x, y, -z + 1/2$
O2	H21	O12	0.96	1.74(1)	2.699(14)	174	$x - 1/2, -y + 1/2, z - 1/2$
O2	H22	O23	0.96	1.76(1)	2.709(13)	169	$-x, -y, -z + 1$
O3	H31	O11	0.96	1.76(1)	2.654(13)	153	$-x + 1/2, y - 1/2, -z + 3/2$
O3	H32	O33	0.96	1.73(1)	2.694(14)	179	$x + 1/2, -y + 1/2, z + 1/2$

[a] Restricted variations, see Experimental section.

Table 3 EXAFS studies of the solid compounds **1** and **2**. Mean bond distances, d, displacement parameters, σ, number of distances, N, the shift in the threshold energy, ΔE_o, and the amplitude reduction factor, S_o^2

Sample	Interaction	N	d/Å	σ/Å	ΔE_o/eV	S_o^2	k-range
1	Hg–O	2	2.111(3)	0.064(3)	−12.9(5)	0.76(5)	2–14
	Hg–O	4	2.474(7)	0.135(4)	−12.9		
	MS[a]	2 × 2	4.21(3)	0.13(4)	−12.9		
2	Tl–O	6	2.205(2)	0.062(3)	−8.7(3)	0.48(1)	2–12
	Tl–O–O	24	3.76(3)	0.11(3)	−8.7		
	MS[b]	3 × 6	4.41(3)	0.14(4)	−8.7		
	Tl ··· S	3	3.40(2)	0.14(1)	−8.7		

[a] The linear multiple scattering paths, Hg–O–O and Hg–O–Hg–O have been refined with a common value for the structural parameters (d, σ and N). [b] The Tl–O–O and two different Tl–O–Tl–O multiple scattering pathways, have been refined with a common value for the structural parameters (d, σ and N).

EXAFS

Mercury and thallium L_3-edge X-ray absorption data were measured at the Stanford Synchrotron Radiation Laboratory (SSRL) using the wiggler beam line 4–1, which was equipped with a Si[220] double crystal monochromator. SSRL operates at 3.0 GeV and a maximum current of 100 mA. The data collection was performed in transmission mode at ambient temperature, and higher order harmonics were rejected by detuning the second monochromator crystal to 50% of maximum intensity at the end of the scans. The solids were diluted with boron nitride powder to give an absorption edge step of about one unit in the logarithmic intensity ratio. The energy scales of the X-ray absorption spectra were calibrated by simultaneously measuring an amalgamated tin or a thallium metal foil as internal standard. The first inflection point of the mercury and thallium metal L_3-edges was set to 12284 and 12660 eV, respectively.[21] After energy calibration, 3–4 scans were averaged for each sample. The EXAFSPAK program package was used for the data treatment.[22] The EXAFS oscillations were obtained after performing standard procedures for pre-edge subtraction, normalisation and spline removal.[23,24] The k^3-weighted EXAFS functions were curve-fitted in k-space using model functions composed of single and multiple scattering pathways calculated from *ab initio* derived phase and amplitude parameters obtained from the FEFF7 program.[25] The input files to FEFF7 were compiled from the corresponding crystal structure data, to contain the Cartesian coordinates of all atoms within a radius of 5 Å from the absorbing metal center.

The standard deviations given for the refined parameters in Table 3, are those obtained from k^3 weighted least squares refinements of the EXAFS function $\chi(k)$, and do not include systematic errors of the measurements. These estimated errors provide a measure of the precision of the results and are useful for comparisons, *e.g.* of relative shifts in the distances. However, the variations in the refined parameters, including the shift in the E_o value (defining $k = 0$), using different models and data ranges, indicate that the accuracy of the distances is within ± 0.01 to 0.02 Å for well-defined interactions. The "standard deviations" given in the text have been increased accordingly to include estimated additional effects of the systematic errors.

Raman and infrared spectra

Raman spectra for the solids **1** and **2** were obtained using a Renishaw 1000 spectrometer, equipped with a Leica DMLM microscope, a 25 mW diode laser (780 nm), and a Peltier-cooled CCD detector. The mid-infrared absorption spectra were obtained by means of a Perkin-Elmer 1720 FT-IR spectrometer (Nujol mull and BaF_2 windows). The far-infrared spectra were recorded by means of a Bio-RAD FTS 6000 FT-IR spectrometer with the sample enclosed between polyethylene disks. Normal coordinate analyses of the spectra and force field calculations were performed by means of Wilson's GF matrix method. A PC-based program package developed by J. and L. Mink[26] was used to compute force constants and to fit calculated vibrational frequencies, using a symmetrised valence force field (symmetry coordinates are given in Table S1).

Results and discussion

Crystal structure of 1

The mercury(II) ion binds strongly two water molecules at a mean Hg–O bond distance of 2.11 Å in an almost linear $Hg(OH_2)_2^{2+}$ entity, O–Hg–O angle 179.0(2)°. Four oxygen atoms from four trifluoromethanesulfonate ions complete a compressed octahedral coordination at a fairly long mean

Hg–O bond distance, 2.53 Å (Fig. 1). Two oxygen atoms of each trifluoromethanesulfonate ion bind to two different $Hg(OH_2)_2^{2+}$ ions forming double bridges in infinite chains, $>Hg(OH_2)_2^{2+}<(CF_3SO_3^-)_2>Hg(OH_2)_2^{2+}<$, along the *ab*-diagonal of the unit cell. The water molecules form fairly strong hydrogen bonds to the sulfonate oxygen atoms of neighbouring chains, giving rise to sheets from which the CF_3 groups protrude (Fig. 2). These sheets are then held together merely by van der Waals interactions between the fluorine atoms, which explains the ease with which the crystals split into flakes (Fig. 3).

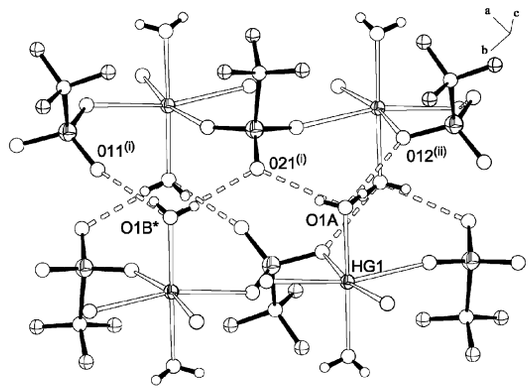

Fig. 2 Two hydrogen bonds (dashes) from each water ligand of the $Hg(OH_2)_2^{2+}$ entities (black Hg–O(aq) bonds) to oxygen atoms of the trifluoromethanesulfonate ions connect the $[Hg(OH_2)_2(O_3SCF_3)_2]_\infty$ chains into layers. Symmetry codes in figure: (*) $-x, -y, -z$; (i) $1 + x, y, z$; (ii) $x, y - 1, z$.

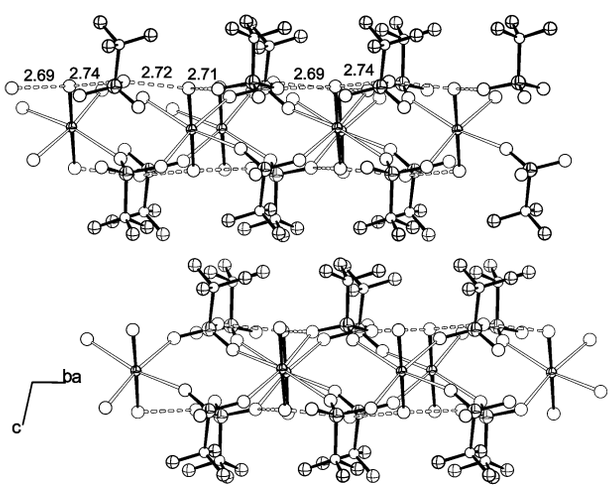

Fig. 3 The layers of **1**, formed by hydrogen bonding between $[Hg(OH_2)_2(O_3SCF_3)_2]_\infty$ chains, are held together merely by van der Waals interactions.

Examination of Figs. 1 and 3 shows that the thermal ellipsoids of the $Hg(OH_2)_2^{2+}$ unit are elongated perpendicular to the layers, an indication of some disorder or twinning in the crystal probably induced by the weak forces between the layers. However, the good agreement between the EXAFS and crystallographic Hg–O(aq) mean bond distances shows that the disorder has not influenced the atom positions in the crystal structure significantly.

This is the first report of an $Hg(OH_2)_2^{2+}$ structure. A fairly large number of crystal structures contain linear O–Hg–O groups, but all are either complexes with oxygen donor ligands, hydroxo and/or oxy groups.[27] The mean Hg–O bond distance in the $Hg(OH_2)_2^{2+}$ entity, 2.11 Å, is similar to distances previously found for linear and pseudo-linear complexes with oxygen donor ligands, such as hydroxide, sulfate, chromate and hydrogen phosphate,[28–36] while the Hg–O bond distances in mercury(II) oxide[37] and in other mercury(II) oxy species,[27,38] are shorter, *ca.* 2.05 Å.

The EXAFS results for **1** indicated the unusual coordination before a single crystal was found which could be used for a crystallographic study (Table 3, Figs. 4a and 5). The

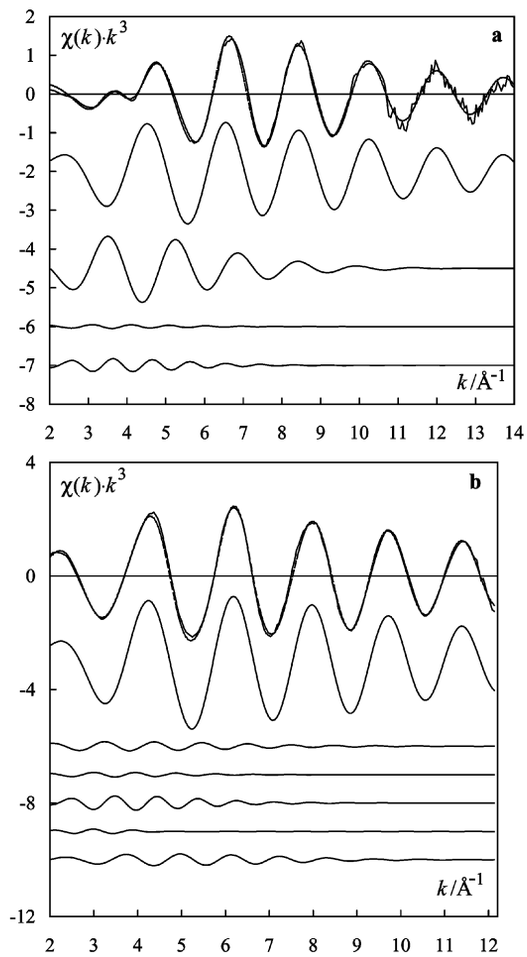

Fig. 4 EXAFS spectra of (**a**): **1** (top) solid line, experimental data and dashed line, model; (below) separate model contributions (*cf.* Table 3): Hg–$2O_{aq}$ (offset −2); Hg–$4O_{trif}$ (offset −4.5), linear multiple scattering Hg–O–O (offset −6) and Hg–O–Hg–O (offset −7); (**b**): **2** (top) solid line, experimental data and dashed line, model; (below) separate contributions: Tl–O (offset −3), multiple scattering Tl–O–O triangular (offset −6), Tl–O–O linear (offset −7), Tl–O–Tl–O linear (offset −8), Tl–O–Tl–O (offset −9) and single scattering Tl ··· S (offset −10).

Debye–Waller factor of the Hg–O bond in the $Hg(OH_2)_2^{2+}$ entity is much smaller than that for the hexahydrate, and is of the same order of magnitude as found for hydrated trivalent metal ions, *cf.* the Debye–Waller factor of **2** in Table 3. Also, the pre-edge structure of the X-ray absorption spectra was indicative of linearity. Fig. S1 shows a more pronounced pre-peak at 12 287 eV for **1** than for $Hg(OH_2)_6(ClO_4)_2$, while the pre-edge structure of **2** is quite similar to that of the $[Tl(H_2O)_6]^{3+}$ ion in aqueous solution (Fig. S2).

The hexahydrated mercury(II) ion, $[Hg(OH_2)_6]^{2+}$, with the mean Hg–O bond distance 2.34 Å,[1,6] hydrolyses to some extent in aqueous solution to $[Hg(OH)(aq)]^+$ and to probably linear $[Hg(OH)_2(aq)]$ complexes, with the second acidity constant larger than the first one, because of the coordination change (pK_{a1} *ca.* 3.4 and pK_{a2} 2.7).[39] For an $Hg(OH_2)_2^{2+}$ entity an even stronger tendency to hydrolysis is expected, because the first hydrolysis constant would be larger for the strongly coordinated water molecules. Thus, the $Hg(OH_2)_2^{2+}$ entity will be stable only in solids with a suitable counter ion or possibly in non-aqueous super acids.

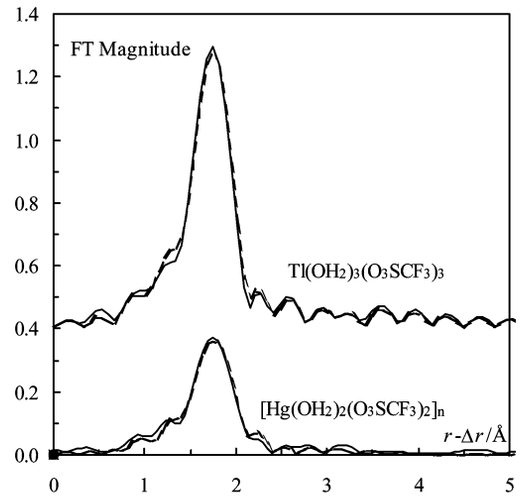

Fig. 5 The Fourier transforms of experimental EXAFS spectra (solid line) and the model function of **1** (bottom) and **2** (offset 0.4). Note the reduced amplitude of **1** due to destructive interference between the EXAFS contributions from the two different groups of Hg–O distances (*cf*. Fig. 4a). The minor multiple scattering and Tl–S contributions of **2** (*cf*. Fig. 4b) are not visible above the Fourier transform truncation ripples of the major Tl–O contribution.

Crystal structure of 2

The crystal structure of **2** is built up of discrete trisaquatris-(trifluoromethanesulfonato)thallium(III) molecular complexes with thallium(III) coordinating six oxygen atoms in octahedral fashion, three from water molecules and three from trifluoromethanesulfonate ions (Fig. 6). The EXAFS data give the

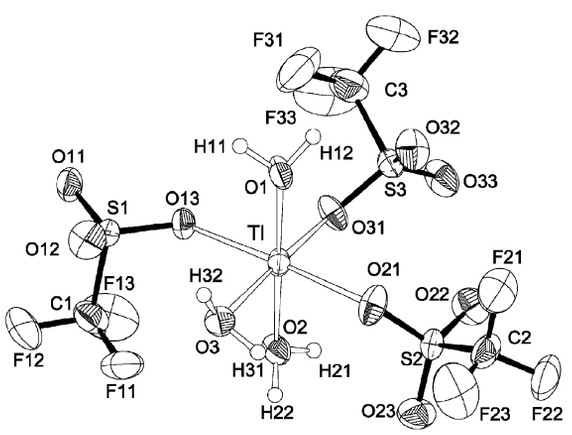

Fig. 6 The molecular structure of **2**. The Tl–O bond distances to the aqua ligands are: Tl1–O1 2.181(9), Tl1–O2 2.217(9), Tl1–O3 2.190(9) Å, and to trifluoromethanesulfonate oxygen atoms: Tl1–O13 2.235(8), Tl1–O21 2.225(9) and Tl1–O31 2.190(9) Å. Thermal ellipsoids at 50 % probability level.

mean Tl–O bond distance 2.205(2) Å, consistent with the crystallographic mean value 2.21 Å (Table 3), and with previous determinations of the hexahydrated thallium(III) ion in aqueous solution and the solid state, *ca*. 2.21 Å.[12,14] The mean Tl–O bond distances for other octahedrally oxygen-coordinated thallium(III) complexes in the solid state are $Cs[Tl(OH_2)_2(SO_4)_2]$ (2.24 Å),[40] $Tl^{I}_{2}Tl^{III}OH(SO_4)_2$ (2.24 Å),[41] $TlOHSO_4 \cdot 2.5\ H_2O$ (2.22 Å)[42] and Tl_2O_3 (2.27 Å).[43]

The mean Tl–O–S bond angle in **2**, 132.9°, is smaller than the corresponding Hg–O–S angle in **1**, 137.1°. Also, the mean O–S–C angle for the coordinated oxygen atoms in the trifluoromethanesulfonate ion, is smaller, 102.0° and 104.7°, respectively, consistent with stronger metal–oxygen bonding for the thallium compound. The average O–(H) · · · O hydrogen bond distance between the water molecules and the trifluoromethanesulfonate ions in **2**, 2.70 Å (Table 2), is similar to that in **1**, 2.71 Å, despite the higher charge on the metal ion.

Vibrational spectra and force constant calculations

Vibrational spectroscopy is a very useful tool to study the bonding character at complex formation. Metal–ligand interactions generally give rise to new bands below 600 cm^{-1}, and the band shifts and splittings of these metal–ligand stretching vibrational modes, as well as of the internal modes of the ligand, may be used to evaluate changes in the M–L bond strength.

The influence of the bonding on the trifluoromethanesulfonate ion was evaluated. As a first step, the force constants were computed for the non-coordinated trifluoromethanesulfonate anion using experimental vibrational spectroscopic data from the literature.[44,45] The trifluoromethanesulfonate ion has C_{3v} point group symmetry (see assignment in Table 4), and its normal vibrations belong to the symmetry species $5A_1 + A_2 + 6E$, all of which except the A_2 torsional mode, are infrared and Raman active fundamentals. The observed and calculated frequencies and potential energy distributions for the normal vibrations of the $CF_3SO_3^-$ anion are summarised in Table S2, while its force constants are presented in Table 4. The results are in fair agreement with those from an *ab initio* study,[46] except for the reversed assignments of the bands at 580 and 520 cm^{-1}.

In order to assess the coordination effects of the trifluoromethanesulfonate complexes a force field study was undertaken of their vibrational spectra. The low-symmetry complexes are rather large for direct evaluations; the Hg-complex has 51 and the Tl-complex 78 vibrational degrees of freedom, even when the water ligands are accounted for as point masses. We have made simplified calculations, firstly accounting for the $O_3SCF_3^-$ ligand coordinated to the metal ion. In the Hg-compound two different oxygen atoms of an $O_3SCF_3^-$ ion form a bridge between two mercury atoms. The two coordinated oxygen atoms have a mean S–O bond length of 1.448 Å, while the third oxygen, which is hydrogen bonded to H_2O molecules, has a shorter S–O bond length, 1.420 Å. In the Tl-complex the $O_3SCF_3^-$ ion coordinates as a monodentate ligand, which gives a longer S–O bond length (1.470 Å). The non-equivalent bonds in the SO_3 group in both cases reduce its local symmetry from C_{3v} to be close to the C_s point group, which leads to 11 A′ and 7 A″ internal vibrational modes for the $O_3SCF_3^-$ ligand.

A second type of calculation has been made for the octahedral coordination sphere with oxygen or water ligands. Around the Hg-atom four SO_3 oxygen atoms form an equatorial plane (O* denotes a coordinated SO_3 oxygen atom) with two *trans*-water molecules in axial positions (see Fig. 1). The point group of this coordination figure is approximately D_{4h}. The coordination sphere of **2** can be described in C_{2v} point group symmetry (*cf.* Fig. 6). The water molecules in the coordination sphere were considered as point masses in all the normal coordinate calculations.

The vibrational spectra of the hexaaqua mercury(II) and thallium(III) complexes were analysed by normal coordinate methods to provide a comparison with the M–O bond strength in the present hydrates. Six experimental and estimated (in brackets) frequencies, 369, (288), 340, 80, (74) and (56) cm^{-1}, have been used for the ν_1 to ν_6 fundamentals of the $[Hg(OH_2)_6]^{2+}$ complex.[46] A similar set of frequencies has been used for $[Tl(OH_2)_6]^{3+}$: 450, 360, 390, (95), (100) and (70) cm^{-1}, respectively.[46] The calculated force constants are summarised in Table 4. The correlation, displayed in Fig. 7a, shows that the force constant decreases substantially with an increase in the M–O bond length with no apparent difference between the mercury(II) and thallium(III) hydrates.

Table 4 Calculated force constants for the $O_3SCF_3^-$ and the $Hg(OH_2)_6^{2+}$ ions, the $Hg(OH_2)_2(O_3SCF_3)_4$ entity (**1**), the $Tl(OH_2)_6^{3+}$ ion, and the $Tl(O_3SCF_3)_3(OH_2)_3$ complex (**2**)

	$O_3SCF_3^-$	$Hg(OH_2)_6^{2+}$	**1**	$Tl(OH_2)_6^{3+}$	**2**
Stretch[a]					
K(CF)	5.758	–	5.758	–	5.758
K(CS)	3.492		3.536		3.427
K(SO)	8.346		9.734		9.417
K(SO*)	–		5.637		3.930
K(MO)	–	1.031	2.502	1.511	1.964
K(MO*)	–		0.966		1.650
Stretch–stretch[a]					
f(CF,CF)	2.607	–	2.576	–	2.607
f(SO,SO)	−0.266		0.0		−0.027
f(SO*,SO*)	–		0.053		–
f(SO,SO*)	–		0.200		−0.050
f(SO*,MO)	–		−0.367		−0.201
f(MO,MO) *cis*	–	0.051	–	0.129	−0.042
f(MO,MO) *trans*	–	0.205	0.628	0.121	0.631
f(MO*,MO*) *cis*	–	–	0.082	–	0.132
f(MO*,MO*) *trans*	–	–	−0.092	–	0.048
Bending[b]					
H(CFC)	1.984	–	1.895	–	1.542
H(FCS)	0.691		0.676		0.908
H(OSO)	2.082		–		1.856
H(OSO*)	–		1.593		1.944
H(O*SO*)	–		1.806		–
H(OSC)	1.230		1.786		1.290
H(O*SC)	–		1.214		1.463
H(OMO)[d]	–	0.112	(0.112)	0.159	(0.159)
Stretch–bend[c]					
h(CF,FCF)	0.460		0.414		0.436
h(CS,FCS)	−0.387		0.474		−0.474
h(MO*,O*S)			−0.218		−0.164
h(MO*,O*SC)			−0.051		−0.063
h(MO,OMO)[d]		(0.046)	(0.046)	(0.046)	(0.046)
Bend–bend[b]					
h(OMO,OMO)[d]		0.010	(0.010)	0.014	(0.014)

Units of the force constants: [a] 10^2 N m^{-1}, [b] 10^{-18} Nm rad^{-2}, [c] 10^{-8} N rad^{-1}, [d] The same force constant is used for all types of oxygen atoms (O* denotes coordinated $O_3SCF_3^-$ oxygen atom).

The $Hg(OH_2)_2(O_3SCF_3)_4$ entity. The experimental and calculated fundamental frequencies are summarised in Table S3. The SO_3 asymmetric and symmetric stretching vibration frequencies of the free $O_3SCF_3^-$ ion shift upon coordination from 1285 to 1280 cm^{-1}, and from 1038 cm^{-1} to 950 cm^{-1} (calculated values), respectively. However, the potential energy distribution shows that the forms of the ligand vibrations have changed drastically in the complex. The band at 1280 cm^{-1} is predominantly the SO stretching mode of the non-coordinated oxygen atom, while the band around 950 cm^{-1} is more characteristic of the symmetric SO_2*-stretching of the SO_2* fragment with the coordinated oxygen atoms. The third band at 1037 cm^{-1} (calculated value) belongs to the asymmetric SO_2* stretching. The formation of a coordination bond *via* the oxygen atoms leads to a decrease of the SO_2* stretching force constant (5.64 N cm^{-1}) as compared to that of the non-coordinated ligand (8.35 N cm^{-1}), while the force constant of non-coordinated SO increases (9.73 N cm^{-1}), because of the additional donor–acceptor interaction between oxygen and sulfur.

The symmetry change due to the coordination of the trifluoromethanesulfonate ligand from the C_{3v} to the C_s point group splits the degenerate E modes into A′ and A″ components. The pairs of bands at 1204/1178, 580/574, 352/349 and 234/218 cm^{-1} correspond to the A′ and A″ species of CF_3 asymmetric stretches (ν_8, ν_8'), SO_3 asymmetric deformations (ν_9, ν_9'), SO_3 rocking (ν_{11}, ν_{11}') and CF_3 rocking (ν_{12}, ν_{12}'), respectively (see Table S3). The central part of the coordination sphere around the Hg atom forms a distorted octahedron, which may be described in D_{4h} symmetry. Then the 15 metal–ligand normal vibrations are classified into $2A_{1g} + B_{1g} + B_{2g} + E_g + 2A_{2u} + B_{1u} + 3E_u$, of which 5 ($2A_{1g}$, B_{1g}, B_{2g}, E_g) vibrations are Raman-active and 5 ($2A_{2u}$, $3E_u$) vibrations are IR-active.

The axial Hg–O bond distance, 2.11 Å, in the $Hg(OH_2)_2^{2+}$ entity is much shorter than that for the $[Hg(OH_2)_6]^{2+}$; complex, 2.34 Å.[1,6] Therefore, both the symmetric and asymmetric Hg–Oax stretching vibrations should be at higher frequency than the averaged Hg–O stretching mode of $[Hg(OH_2)_6]^{2+}$, 328 cm^{-1}. The Raman band at 574 cm^{-1} and the IR band at 410 cm^{-1} were assigned to the A_{1g} and A_{2u} modes of the HgO_2 stretching vibrations, respectively.

The mean equatorial Hg–O* bond distance is 2.53 Å, which suggests an assignment of bands below 328 cm^{-1} for the equatorial HgO_4* stretching vibrations. Consequently, the two Raman bands at 256 and 185 cm^{-1} were assigned to the A_{1g} and B_{2g} HgO_4* stretching vibrations, respectively. The E_u species were observed in the infrared spectrum at 285 cm^{-1}. For deformation modes the calculated frequencies are in the range of 85–50 cm^{-1}.

To further study the hydrogen bonding around the $Hg(OH_2)_2^{2+}$ entity we performed an infrared spectroscopic study of the uncoupled O–D stretching vibrations on the solid bisaquamercury(II) trifluoromethanesulfonate. Isotpic substitution was made by recrystallizing the salt from an aqueous solution with about 5% D_2O.[47] The spectrum shows a

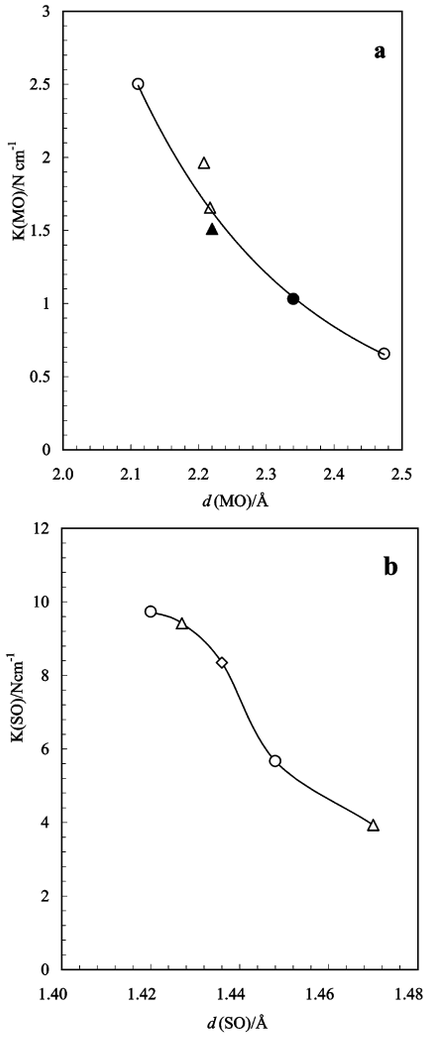

Fig. 7 (**a**) Correlation between metal–oxygen (MO) force constants and bond lengths in **1** (○), **2** (△), $[Hg(OH_2)_6]^{2+}$ (●) and $[Tl(OH_2)_6]^{3+}$ (▲) complexes. (**b**) Correlation between SO force constants, *K*(S–O)/N cm^{-1} (Table 4) from averaged SO_3 stretching frequencies (Tables S2–S4) and bond lengths *d*(S–O)/Å in $O_3SCF_3^-$ ions, free (◇), in **1** (○), and **2** (△).

broad O–D stretching band centered at about 2400 cm^{-1} (ca. 170 cm^{-1} bandwidth). The frequency is considerably lower than that for the O–D stretching of the hexahydrated Hg^{2+} ion in partially deuterated $[Hg((H,D)_2O)_6](ClO_4)_2$(s) at 2567 cm^{-1} (width 106 cm^{-1}), and slightly lower than the O–D band of the $[Hg((H,D)_2O)_6]^{2+}$ ion in aqueous solution, 2416 cm^{-1} (width 193 cm^{-1}).[48] A lower O–D stretching frequency of water molecules indicates a stronger hydrogen bond, and correlates well with a shorter O ⋯ O bond distance, in particular when dilute HOD is used to avoid vibrational coupling.[47–49] The frequency 2400 cm^{-1} corresponds to a mean (O(–H) ⋯ O) distance of about 2.74 ± 0.07 Å, according to a solid state correlation between hydrogen bonded O ⋯ O distances and ν_{OD} wavenumbers.[49] This is in agreement with the crystallographic values (Table 2), with the mean O–(H) ⋯ O distance 2.71 Å. Thus, the strong Hg–O bond in the $Hg(H_2O)_2^{2+}$ entity polarises the coordinated water molecules and enhances the hydrogen bond strength as compared to that in hexahydrated mercury(II) ions, even in aqueous solution.

The $[Tl(OH_2)_3(O_3SCF_3)_3]$ complex. The experimental and calculated fundamental frequencies are summarised in Table S4. In the thallium complex the $O_3SCF_3^-$ ligand is monodentate, with only one oxygen atom (O*) coordinated to thallium. Therefore, the SO_3 group vibrations can be divided into two SO_2 stretchings, asymmetrical (1304 cm^{-1}) and symmetrical (1273 cm^{-1}), and one SO* stretching band at 829 cm^{-1}. The two higher frequencies are close to the degenerate SO_3 stretching mode (ν_7) of the free ligand at 1285 cm^{-1}, and the lower frequency corresponds to the longest SO* distance (1.478 Å). Due to the symmetry lowering the degenerate E modes of the trifluoromethanesulfonate ligand split into two components. The pair of bands at 1180/1154 and 214/192 cm^{-1} refers to CF_3 asymmetric stretching (ν_8, ν_8') and rocking (ν_{12}, ν_{12}') modes of the ligand, respectively.

The octahedral arrangement around the Tl atom comprises three vicinal H_2O groups in a plane and three coordinated oxygen (O*) atoms of $O_3SCF_3^-$ ligands located in a perpendicular plane. Therefore, the coordination sphere of the thallium atom may be described in C_{2v} symmetry (Fig. 6). With this description, the 15 metal–ligand normal modes belong to the $6A_1 + A_2 + 4B_1 + 4B_2$ symmetry species. The metal–oxygen bond lengths are slightly shorter in this TlO_6 entity than in the $[Tl(OH_2)_6]^{3+}$ complex. The bands at 519, 375 and 347 cm^{-1} were assigned to the three Tl–O stretching modes, belonging to the A_1, B_1 and A_1 symmetry species of the C_{2v} point group, respectively (see Table S4).

Three bands at 432, 397 and 355 cm^{-1} can be assigned to Tl–O* stretching modes belonging to the A_1, B_2 and A_1 symmetry species, respectively. This set of frequencies originate from Tl–O* bonds formed to the coordinated $O_3SCF_3^-$-ligands. The calculated frequencies of the OTlO deformation modes ($2A_1 + A_2 + 3B_1 + 3B_2$) are in the range 76–98 cm^{-1} (see Table S4).

Force constants. The SO_3 group of the triflate ion showed geometrical changes due to the coordination. For a strong M–O bond the S–O bond distance increases, while the non-coordinated S–O bond lengths decrease. The correlation presented in Fig. 7b between the S–O force constants and corresponding S–O bond distances show that while the S–O bond distances vary from 1.420 to 1.470 Å, the force constants decrease more drastically, from 9.7 to 3.9 N cm^{-1} (Table 4).

Conclusions

Bisaquamercury(II) trifluoromethanesulfonate, $[Hg(OH_2)_2(CF_3SO_3)_2]_\infty$, shows an unusual connectivity with covalently bonded nearly linear bisaquamercury(II) entities, $Hg(OH_2)_2^{2+}$, mean Hg–O(aq) bond distance 2.11 Å, held together in $Hg(OH_2)_2(CF_3SO_3)_2$ chains by bridging trifluoromethanesulfonate ions. Double bridges are formed *via* two of the oxygen atoms of the SO_3 group with four much weaker Hg–O bonds, mean distance 2.53 Å. The polarisation of the two strongly bound water ligands in a $Hg(OH_2)_2^{2+}$ entity leads to relatively strong hydrogen bonding holding the parallel chains together in layers, from which the CF_3 groups protrude. The layers are loosely held together by van der Waals contacts between the CF_3 groups, giving the crystalline compound a fragile sheet structure.

For safety reasons, especially for non-aqueous solutions, trifluoromethanesulfonate salts are often recommended instead of perchlorate, and the trifluoromethanesulfonate ion is regarded as having a low tendency to form ion pairs with metal ions. However, previous studies show that silver(I) and mercury(II) trifluoromethanesulfonate salts are reduced in some solvents with strong electron-pair donating properties, such as *N,N*-dimethylthioformamide[10,50] and liquid ammonia, while corresponding perchlorate solutions of salts with fully solvated metal ions do not decompose. Note, however, that incomplete solvation during preparation can give violent explosions, probably caused by direct metal–perchlorate bonding.[50]

The present study shows that the trifluoromethanesulfonate ion, in contrast to perchlorate, can replace water ligands in the hexaaqua ions of mercury(II) and thallium(III) when the

hydrated salts crystallise. The thallium(III) ion retains an almost regular octahedral coordination of the oxygen atoms. However, mercury(II), which is much more strongly influenced by SOJT effects, shows a pronounced change in coordination geometry from a more or less regular six-coordination in solution to a 2 + 4 configuration in the solid hydrated compound. It seems reasonable that the low stability of mercury(II) trifluoromethanesulfonate in some non-aqueous solvents is connected to SOJT-induced coordination changes, allowing direct coordination of the trifluoromethanesulfonate and mercury(II) ions.

Acknowledgements

Financial support from the Swedish Research Council, the Wenner–Gren Foundations and the Hungarian National Research Foundation (OTKA T025278) is gratefully acknowledged. The EXAFS measurements were carried out at the Stanford Synchrotron Radiation Laboratory, a national user facility operated by Stanford University on behalf of the U.S. Department of Energy, Office of Basic Energy Sciences. The SSRL Structural Molecular Biology Program is supported by the Department of Energy, Office of Biological and Environmental Research, and by the National Institutes of Health, National Center for Research Resources, Biomedical Technology Program.

References

1 G. Johansson and M. Sandström, *Acta Chem. Scand., Ser. A*, 1978, **32**, 109.
2 M. Sandström and I. Persson, *Acta Chem. Scand., Ser. A*, 1978, **32**, 95.
3 J. M. Hook, P. A. W. Dean and D. C. R. Hockless, *Acta Crystallogr., Sect. C*, 1995, **51**, 1547.
4 D. L. Kepert, D. Taylor and A. H. White, *J. Chem. Soc., Dalton Trans.*, 1973, 670.
5 R. Åkesson, M. Sandström, C. I. Stålhandske and I. Persson, *Acta Chem. Scand.*, 1991, **45**, 165.
6 P. Lindqvist-Reis, S. Pattanaik, I. Persson P. Persson and M. Sandström, *Inorg. Chem.*, submitted.
7 M. Sandström, I. Persson and S. Ahrland, *Acta Chem. Scand., Ser. A*, 1978, **32**, 607.
8 I. B. Bersuker, *The Jahn-Teller Effect and Vibronic Interactions in Modern Chemistry*, Plenum, New York, 1984, ch. 1–5.
9 M. Sandström, I. Persson and P. Persson, *Acta Chem. Scand.*, 1990, **44**, 653.
10 C. M. V. Stålhandske, I. Persson, M. Sandström and E. Kamienska-Piotrowicz, *Inorg. Chem.*, 1997, **36**, 3174.
11 K. B. Nilsson, M. Maliarik, I. Persson and M. Sandström, unpublished work (data available: Ingmar.Persson@kemi.slu.se).
12 J. Glaser and G. Johansson, *Acta Chem. Scand., Ser. A*, 1981, **35**, 639.
13 J. Blixt, J. Glaser, J. Mink, I. Persson, P. Persson and M. Sandström, *J. Am. Chem. Soc.*, 1995, **117**, 5089 and references therein.
14 G. Ma, A. Molla-Abbassi, M. Kritikos, A. Ilyukhin, F. Jalilehvand, V. Kessler, M. Skripkin, M. Sandström, J. Glaser, J. Näslund and I. Persson, *Inorg. Chem.*, 2001, **40**, 6432.
15 J. Glaser and G. Johansson, *Acta Chem. Scand., Ser. A*, 1982, **36**, 125.
16 A. Linden, A. Petridis and B. D. James, *Inorg. Chim. Acta*, 2002, **332**, 61 and references therein.
17 I. Persson, F. Jalilehvand and M. Sandström, *Inorg. Chem.*, 2002, **41**, 192.
18 (*a*) STOE Image Plate Diffractometer Software (IPDS), version 2.87, STOE & Cie GmbH, Darmstadt, 1997; (*b*) Bruker SMART and SAINT, area detector control and integration software, Bruker Analytical X-ray Systems, Madison, WI, 1995.
19 (*a*) X-SHAPE version 1.02; (*b*) X-RED version 1.09, STOE & Cie GmbH, Darmstadt, 1997.
20 G. M. Sheldrick, *Acta Crystallogr., Sect. A*, 1990, **46**, 467.
21 A. Thompson, D. Attwood, E. Gullikson, M. Howells, K.-J. Kim, J. Kirz, J. Kortright, I. Lindau, P. Pianatta, A. Robinson, J. Scofield, J. Underwood, G. Vaughan, Williams and H. Winick *X-ray Data Booklet, LBNL/PUB-490 Rev. 2*, Lawrence Berkeley National Laboratory, Berkeley, CA, 2001.
22 G. N. George and I. J. Pickering *EXAFSPAK – A Suite of Computer Programs for EXAFS Analysis*, SSRL, Stanford University, CA, 1993.
23 The theory and procedure is described in: F. Jalilehvand, Structure of Hydrated Ions and Cyano Complexes by X-Ray Absorption Spectrosocpy, Doctoral Thesis, Royal Institute of Technology, Stockholm, 2000; http://media.lib.kth.se:8080/dissengrefhit.asp?dissnr=296.
24 S. P. Cramer, K. O. Hodgson, E. I. Stiefel and W. E. Newton, *J. Am. Chem. Soc.*, 1978, **100**, 2748.
25 S. I. Zabinsky, J. J. Rehr, A. Ankudinov, R. C. Albers and M. J. Eller, *Phys. Rev. B*, 1995, **52**, 2995.
26 J. Mink and L. M. Mink *Computer Program System for Vibrational Analyses of Polyatomic Molecules*, Technical Report, Erlangen and Stockholm 1993; available from Professor J. Mink, Institute of Isotopes and Surface Chemistry, Chemical Research Center of the Hungarian Academy of Sciences, P.O. Box 77, H-1525, Budapest, Hungary.
27 *Inorganic Crystal Structure Data Base*, Gmelin Institut, Fachinformationszentrum, Karlsruhe, release 98/1.
28 B. Ribar, M. Matkovic, M. Sljukic and F. Gabela, *Z. Kristallogr., Kristallgeom., Kristallphys., Kristallchem.*, 1971, **134**, 311.
29 M. Matkovic, B. Ribar, B. Prelesnik and R. Herak, *Inorg. Chem.*, 1974, **13**, 3006.
30 G. Björnlund, *Acta Chem. Scand.*, 1971, **25**, 1645.
31 C. Stålhandske, *Acta Crystallogr., Sect. B*, 1980, **36**, 23.
32 K. Aurivillius and C. Stålhandske, *Z. Kristallogr., Kristallgeom., Kristallphys., Kristallchem.*, 1976, **144**, 1.
33 G. Björnlund, *Acta Chem. Scand., Ser. A*, 1974, **28**, 169.
34 N. I. Galovastikov, *Kristallografiya*, 1984, **29**, 604.
35 K. Aurivillius and C. Stålhandske, *Z. Kristallogr., Kristallgeom., Kristallphys., Kristallchem.*, 1975, **142**, 129.
36 E. Dubler, L. Beck, L. Linowsky and G. B. Jameson, *Acta Crystallogr., Sect. B*, 1981, **37**, 2214.
37 (*a*) K. Aurivillius and I. B. Carlsson, *Acta Chem. Scand.*, 1958, **12**, 1297; (*b*) K. Aurivillius and I. B. Carlsson, *Acta Chem. Scand.*, 1957, **11**, 1069; (*c*) K. Aurivillius and I. B. Carlsson, *Acta Chem. Scand.*, 1964, **18**, 1305.
38 G. Johansson and E. Hansen, *Acta Chem. Scand.*, 1972, **26**, 726.
39 The IUPAC Stability Constants Database, Academic Software, Otley, 2000, and references therein.
40 J. M. Manoli, P. Herpin and A. Dereigne, *Acta Crystallogr., Sect. B*, 1972, **28**, 806.
41 F. Abraham, G. Nowogroicki, B. Jolibois and G. Laplace, *J. Solid State Chem.*, 1983, **47**, 1.
42 G. Johansson, *Acta Chem. Scand.*, 1959, **13**, 925.
43 H. H. Otto, R. Baltrush, H.-J. Brandt and P. Papamantellos, *Z. Kristallogr., Kristallgeom., Kristallphys., Kristallchem.*, 1968, **126**, 143.
44 M. G. Miles, G. Doyle, R. P. Corney and R. S. Tobias, *Spectrochim. Acta, Sect. A*, 1969, **25**, 1515.
45 G. Shridjar, K. Hermansson and J. Lindgren, *J. Phys. Chem.*, 1994, **98**, 8687.
46 C. Carr, PhD Thesis, University of Bristol, 1984, pp. 67 and 113.
47 O. Kristiansson, J. Lindgren and J. de Villepin, *J. Phys. Chem.*, 1988, **92**, 2680.
48 P.-Å. Bergström, J. Lindgren, M. Sandström and Y. Zhou, *Inorg. Chem.*, 1992, **31**, 150.
49 B. Berglund, J. Lindgren and J. Tegenfeldt, *J. Mol. Struct.*, 1978, **43**, 179.
50 C. M. V. Stålhandske, C. I. Stålhandske, I. Persson, M. Sandström and F. Jalilehvand, *Inorg. Chem.*, 2001, **40**, 6684.